Optica Applicata, Vol. XXXII, No. 3, 2002

Numerical modelling of InGaAs infrared photovoltaic detectors

MAREK SIOMA

Warsaw University of Technology, ul. Koszykowa 75, 06–662 Warszawa, Poland.

JANUSZ KANIEWSKI

Institute of Electron Technology, al. Lotników 32/46, 02–668 Warszawa, Poland.

The performance of p-i-n infrared detectors has been studied theoretically. Optimization of $In_xGa_{1-x}As$ device structure has been performed for three compositions, $x = 0.53$, $x = 0.82$ and $x = 1$, which are important from the application point of view. Calculations have been performed by means of APSYS simulation program and the model based on fundamental limitations to the detector operation. The influence of layer thickness, as well as doping concentration in the active layer on zero bias resistance and detectivity of devices optimized for desired cut-off wavelength have been discussed. Additionally, the photovoltaic effect across the structure has been discussed. Finally, the influence of the ohmic contact position on photodiode parameters has been shown.

1. Introduction

The $In_xGa_{1-x}As$ ternary alloys cover a wide range of lattice constants a between the GaAs one ($x = 0$: $a = 0.5653$ nm, $E_g = 1.43$ eV) and the InAs lattice constant ($x = 1$: $a = 0.6058$ nm, $E_g = 0.35$ eV). Except the alloy composition $In_{0.53}Ga_{0.47}As$, which is lattice-matched to InP, all other $In_xGa_{1-x}As$ compounds grown on GaAs or InP substrates are mismatched materials. Therefore, the quality of $In_xGa_{1-x}As$ based devices is often limited by the presence of mismatch dislocations [1], [2]. Nevertheless, InGaAs is still a very attractive material for near-infrared detectors. They can operate in $1-3.6$ μm spectral region. InGaAs based detectors are alternative to PbS ones which suffer from instability problems, and antimony containing structures. The devices can be used for detection of thermal radiation emitted by objects at elevated temperatures, for environmental sensing of atmospheric constituents such as CO_2, CO, CH_4 and many others. Modern III – V compounds technology makes it possible to grow heterostructures with a complex gap and doping profiles which are necessary to achieve a good performance. Therefore, intensive modelling is strongly needed in optimizing the devices [3], [4].

2. Theoretical analysis and detector structure

Intensive calculations of the detector structure have been performed by using the commercially available simulation program APSYS developed by Crosslight Software Inc. APSYS is the two-dimensional finite element analysis that solves self -consistently the Poissons's equation and current continuity equations for electrons and holes. In the calculations Shockley–Read–Hall recombination processes, as well as Auger non-radiative processes, are taken into account [5]. Additionally, numerical modelling based on fundamental limitations of the detector operation has been performed [3], [6], [7]. In the model applied it has been assumed after PIOTROWSKI *et al.* [3], [4], [8] that the best detectivity D^*, of the detector is obtained when $t = 1.26/\alpha$, where t is the active layer thickness and α is the absorption coefficient, The value of α has been calculated according to Kane's model [9]. In the calculations the Fermi level position has been taken into account.

In the analysis, an important detector parameter, the so-called R_0A product (zero bias differential resistance R_0 times detector area A) has been calculated. Simultaneously, a simple relation between detectivity D^* and R_0A product has been applied [10]

$$D^* = \frac{q}{E_g}\sqrt{\frac{R_0A}{4kT}} \tag{1}$$

where: q – electronic charge, E_g – energy gap, k – Boltzmann's constant, T – temperature.

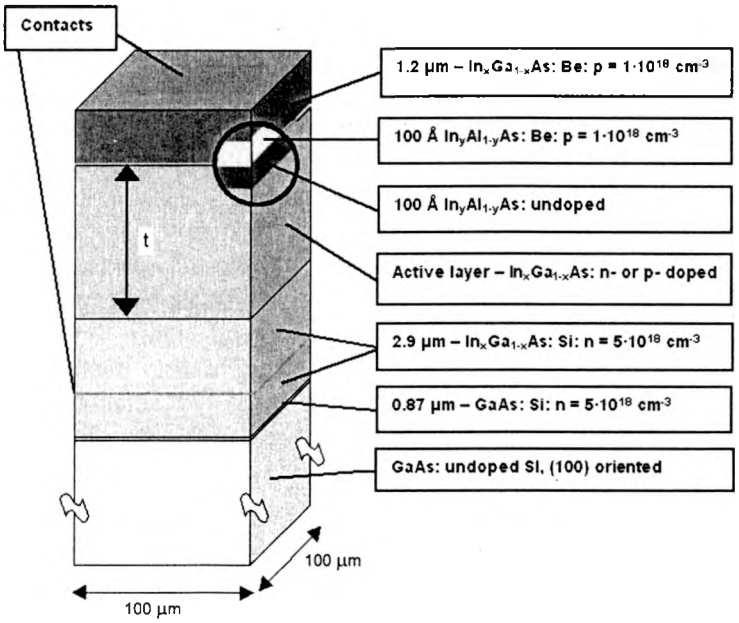

Fig. 1. Schematic cross-section of InGaAs detector structure – type II.

In the simulations, all material parameters have been assumed after [11], [12]. Auger coefficients and lifetimes for electrons and holes have been estimated by fitting the theoretical device characteristics to experimental ones.

Two types of detector structures, labeled type I and type II, have been considered. They differed by very thin barrier layers only. The InAlAs layers were present in the structure type II, as it is shown in Fig. 1, whereas in the structure type II they were omitted. The energy gap of thin InAlAs layers was wider than that of InGaAs layers in the structure.

Calculations have been performed for detectors with n-type or p-type active layers doped to different levels. In the analysis of the ohmic contact position it has been assumed that distance from 100×100 μm^2 mesa structure changes from 0 to 300 μm.

3. Results and discussion

Figure 2 shows R_0A product values for three compositions of $In_xGa_{1-x}As$ detector structures, $x = 0.53$, $x = 0.82$ and $x = 1$. The results have been obtained from APSYS simulations. It is seen that the value of R_0A is smaller for devices that operate at longer wavelength. As it results from Eq. (1) one can expect that detectivities D^*, of devices operating at longer wavelength are also significantly smaller. This is consistent with previous theoretical predictions and experimental results [3], [4], [11].

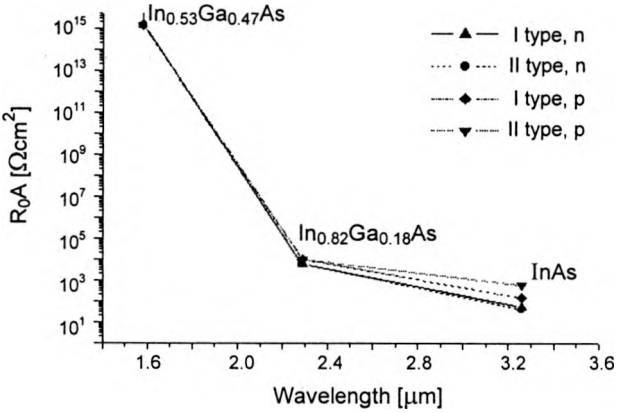

Fig. 2. R_0A product for InGaAs detectors optimized for different wavelengths.

In order to determine the thickness of the active layer in the optimized devices additional calculations have been performed. The model based on fundamental limitations of the detector operation has been applied. In the analysis, the changes in active layer composition and doping level have been considered. The results are presented in Figs. 3 and 4. It is seen that in the detectors optimized for long wavelength operation almost 7 μm thick active layer is required. In the case of detectors optimized for 1.6 μm operation the thickness of the active layer should be

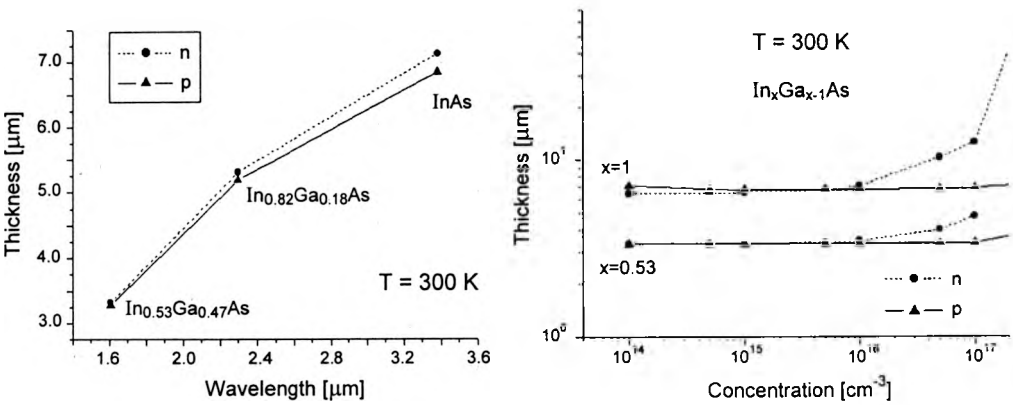

▲

Fig. 3. Thickness of the active layer for InGaAs detectors optimized for different wavelength.

Fig. 4. Thickness of the active layer of optimized $In_xGa_{1-x}As$, $x = 1$ and $x = 0.53$ photovoltaic detectors as a function of carrier concentration.

about 3.5 μm. On the other hand, this thickness remains constant for low doping and is similar for n-type and p-type layer (Fig. 4). The optimum thickness of the heavily doped ($n > 1 \times 10^{16}\,cm^{-3}$) n-type active layer increases with doping as a result of reduced absorption due to the Burstein–Moss effect. In contrast the optimum thickness of p-type active layer is independent of doping level. Sumarizing, one can conclude, that the optimum active layer thickness increases with decreasing band gap and it is roughly equal to the double wavelength for which the devices is optimized.

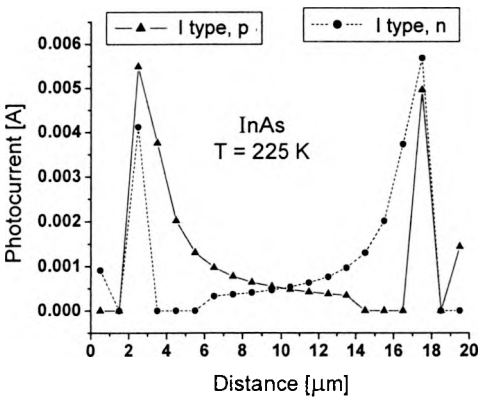

Fig. 5. Photovoltaic signal across InAs detector structure as determined from APSYS simulations.

Changes of photovoltaic effect across hypothetical p-i-n detector structure have been considered by means of APSYS software. In the calculations it has been assumed that the photocurrent is measured locally and the active layer is extremely

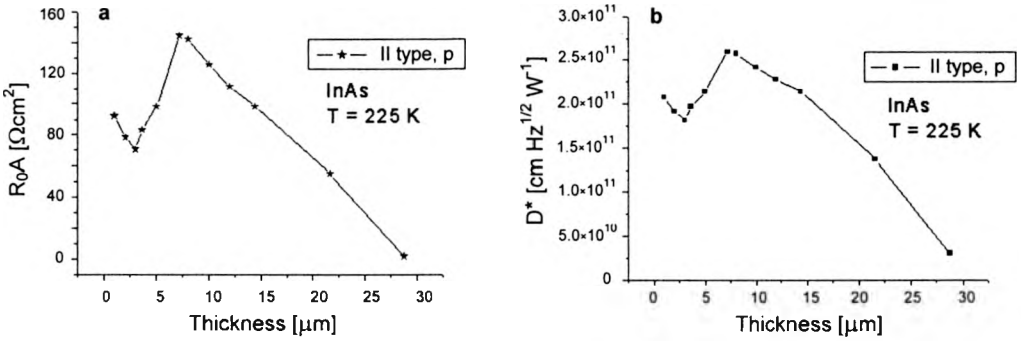

Fig. 6. Calculated parameters of InAs photovoltaic detector (type II) as a function of the active layer thickness: **a** – for R_0A product, **b** – for detectivity D^*.

thick. The results are presented in Fig. 5. No important differences with respect to the photocurrent have been found for n-type and p-type active layer. However, the value of the photocurrent at the p-n interface is surprisingly similar to the one calculated for the active layer–contact layer interface, *i.e.*, high (concentration)–low (concentration) interface.

It is known that the active layer thickness plays a very important role in optimization of the detector structure. Changes of R_0A and D^*, for InAs devices calculated using APSYS simulations are presented in Fig. 6. The optimized thickness of an active layer for InAs detectors, which can operate up to 3.6 μm, amounts to 7 μm [4]. This agrees well with the result of previously discussed simulations based on fundamental limitations of the detector performance (see Fig. 3).

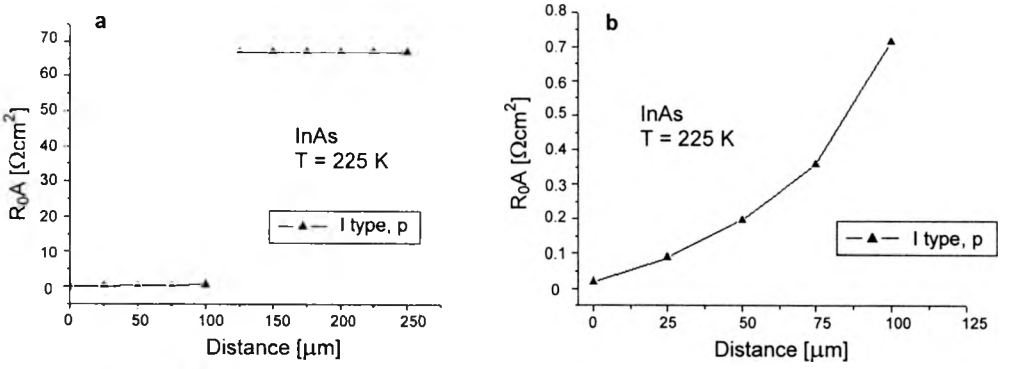

Fig. 7. Changes of R_0A as a function of distance from the ohmic contact to mesa edge; **a** – at the distance greater than 125 μm contact is on highly doped (5×10^{-18} cm^{-3}) layer, **b** – at the distance less than 125 μm is confined to the active layer.

During processing the detector structures the well-defined shape of a mesa structure is highly important. Using APSYS program the changes of detector parameters resulting from failures in etching procedure has been simulated. It has

been assumed that the mesa structure has not been completely defined and a part of contact metalization is put on the active layer. The effect is clearly seen in Fig. 7. In this situation, the degradation of the R_0A product values is immediate. Good device parameters can be obtained when metalization is confined to highly doped n-InAs layer [13].

4. Conclusions

Important parameters of InGaAs photovoltaic detectors have been calculated. It has been found that the value of R_0A product changes from about $1 \times 10^{15}\ \Omega\text{cm}^2$ for devices operating at 1.6 μm to about $1 \times 10^{2}\ \Omega\text{cm}^2$ for detectors operating at 3.3 μm.

Generally, it is required that the carrier concentration in optimized devices has to be lower than $1 \times 10^{16}\ \text{cm}^{-3}$ and the optimum active layer thickness increases with decreasing band gap and is roughly equal to the double wavelength for which the device is optimized.

It has been found that detector performance is completely degraded due to failures in the mesa structure definition.

Acknowledgments – The work was partially supported by the State Committee for Scientific Research (KBN), Poland, grant No. 8 T11B 029 21.

References

[1] KANIEWSKI J., ORMAN Z., PIOTROWSKI J., REGIŃSKI K., ROMANIS M., Proc. SPIE **4130** (2000), 749.
[2] KANIEWSKI J., ORMAN Z., PIOTROWSKI J., SIOMA M., ORNOCH L., ROMANIS M., Proc. SPIE **4369** (2001), 721.
[3] PIOTROWSKI J., KANIEWSKI J., IEE Proc. Optoelectron. **146** (1999), 173.
[4] PIOTROWSKI J., KANIEWSKI J., REGIŃSKI K., Nucl. Instrum. Methods Phys. Res., Sect. A **439** (2000), 647.
[5] *APSYS User's Manual*, Part I: *Description*, version 3.6, 1995–2000, Crosslight Software Inc.
[6] BIELECKI Z., ROGALSKI A., *Detection of Optical Signals*, (in Polish), [Ed.] WNT, Warszawa 2001, p. 60.
[7] ROGALSKI A., Infrared Phys. Technol. **41** (2000), 213.
[8] PIOTROWSKI J., GARON W., Infrared Phys. Technol. **38** (1997), 63.
[9] KANE E.O., J. Phys. Chem. Solids **1** (1957), 249.
[10] TIAN Y., ZHOU T., ZHANG B., JIANG H., JIN Y., IEEE Trans. Electron Devices **46** (1999), 656.
[11] ROGALSKI A., CIUPA R., J. Electron. Mater. **28** (1999), 630.
[12] AHRENKIEL R.K., ELLINGSON R., JOHNSTON S., WANLASS M., Appl. Phys. Lett. **72** (1998), 3470.
[13] WENUS J., RUTKOWSKI J., ROGALSKI A., IEEE Trans. Electron Devices **48** (2001), 1326.

Received May 13, 2002